

# Sensing Glove for Brain Studies: Design and Assessment of Its Compatibility for fMRI With a Robust Test

Nicola Vanello, Valentina Hartwig, Mario Tesconi, Emiliano Ricciardi, Alessandro Tognetti, Giuseppe Zupone, Roger Gassert, *Member, IEEE*, Dominique Chapuis, *Member, IEEE*, Nicola Sgambelluri, Enzo P. Scilingo, Giulio Giovannetti, Vincenzo Positano, *Member, IEEE*, Maria F. Santarelli, Antonio Bicchi, *Fellow, IEEE*, Pietro Pietrini, Danilo De Rossi, and Luigi Landini

**Abstract**—In this paper, we describe a biomimetic-fabric-based sensing glove that can be used to monitor hand posture and gesture. Our device is made of a distributed sensor network of piezoresistive conductive elastomers integrated into an elastic fabric. This solution does not affect natural movement and hand gestures, and can be worn for a long time with no discomfort. The glove could be fruitfully employed in behavioral and functional studies with functional MRI (fMRI) during specific tactile or motor tasks. To assess MR compatibility of the system, a statistical test on phantoms is introduced. This test can also be used for testing the compatibility of mechatronic devices designed to produce different stimuli inside the MR environment. We propose a statistical test to evaluate changes in SNR and time-domain standard deviations between image sequences acquired under different experimental conditions. fMRI experiments on subjects wearing the glove are reported. The reproducibility of fMRI results obtained with and without the glove was estimated. A good similarity between the activated regions was found in the two conditions.

**Index Terms**—Brain activity exploration, fabric sensing glove, MRI compatibility, piezoresistive elastomers, statistical test.

## I. INTRODUCTION

**I**N THIS PAPER, we report the results about functional MRI (fMRI) compatibility of a novel sensing glove realized

Manuscript received November 15, 2007; revised February 25, 2008. Recommended by Guest Editor A. Khanicheh. This work was supported by the European Union under Sixth Framework Programme Priority 2 (IST-2006-27141).

N. Vanello and L. Landini are with the Department of Information Engineering, University of Pisa, 56100 Pisa, Italy (e-mail: nicola.vanello@iet.unipi.it; llandini@ifc.cnr.it).

V. Hartwig, M. Tesconi, A. Tognetti, G. Zupone, N. Sgambelluri, E. P. Scilingo, A. Bicchi, and D. De Rossi are with the Interdepartmental Research Center “E. Piaggio,” University of Pisa, 56100 Pisa, Italy (e-mail: valeh@ifc.cnr.it; mario.tesconi@ing.unipi.it; a.tognetti@ing.unipi.it; g.zupone@gmail.com; nicola.sgambelluri@ing.unipi.it; e.scilingo@ing.unipi.it; bicchi@ing.unipi.it; d.derossi@ing.unipi.it).

E. Ricciardi and P. Pietrini are with the Laboratory of Clinical Biochemistry and Molecular Biology, University of Pisa Medical School, I-56126 Pisa, Italy (e-mail: emiliano.ricciardi@bioclinica.unipi.it; pieter.pietrini@bm.med.unipi.it).

R. Gassert is with the Department of Bioengineering, Imperial College London, London, SW7 2AZ, U.K. (e-mail: roger.gassert@imperial.ac.uk).

D. Chapuis is with the Laboratoire de Systèmes Robotiques, Ecole Polytechnique Fédérale de Lausanne (EPFL), 1015 Lausanne, Switzerland (e-mail: dominique.chapuis@epfl.ch).

G. Giovannetti, V. Positano, and M. F. Santarelli are with the MRI Laboratory, Istituto di Fisiologia Clinica (IFC), Consiglio Nazionale delle Ricerche (CNR), 56100 Pisa, Italy (e-mail: giovannetti@ifc.cnr.it; positano@ifc.cnr.it; santarell@ifc.cnr.it).

Color versions of one or more of the figures in this paper are available online at <http://ieeexplore.ieee.org>.

Digital Object Identifier 10.1109/TMECH.2008.924115

with strain sensing fabrics. The glove can be used to monitor hand posture and gesture, and it could be properly used in behavioral and functional studies.

In our realization, sensors and connections are integrated in an elastic textile substrate. They are made by an elastomeric material, and no metallic parts are present on the glove. For this reason, the mechanical properties of the substrate are not modified. The whole system is lighter and more comfortable for the user compared to the “state-of-the-art” instrumented glove, Cyberglove [1]. The user is free to move his/her hands without feeling mechanical constraints, which could interfere with the execution of the task under study. Moreover, the described technology, if used in large-scale production, can dramatically reduce the costs with respect to existing systems on the market.

The aim of this study is to verify whether the information acquired by the sensing glove could be integrated with the fMRI data in order to explore brain networks involved in the execution of tactile or motor tasks. The role of brain areas underlying a specific task execution can be differentiated by improving the characterization of the task performed by a subject during an fMRI experiment. The information acquired from the glove can be used to obtain a detailed description over time of the actual task performed by the subject. This description allows to build an expected time course of blood oxygenation–level-dependent (BOLD) signal changes elicited by the executed task [2].

Another glove has been proposed to be compatible with MRI [3]. It has fiber-optic-based flexion sensors placed on the fingers connected to the acquisition unit through waveguide. No information on the resolution in angle measurements is given in the data sheet.

fMRI-compatible mechatronic devices [4]–[9] have been designed to assure reproducibility, control, and monitoring of visuo-motor performances. Moreover, they have to satisfy safety and compatibility criteria [10].

After describing the proposed glove and its possible applications, a test to assess the compatibility of the system with fMRI investigations is introduced. Previous studies introduced methods for verifying the MR compatibility of materials and for determining device-induced artifacts [4]–[8], [11]–[14]. A simple visual inspection of raw MR data or subtraction images acquired under different experimental conditions, such as device ON/OFF, might be sufficient to detect major artifacts [13]. Conversely, the presence of subtle but significant changes could

require to estimate the changes in the image SNR [4], [11] or assess signal mean value and standard deviation in different regions of interest (ROIs) [7]. Guidelines are provided by the National Electric Manufacturing Association (NEMA) organization to estimate SNR in diagnostic MRI [15]. Time-invariant distortions may be evaluated by acquiring images whose voxel value minimizes the sum of the squares for that voxel's residuals over time [8]. Time-variant changes in the SNR can be assessed by defining a measure of the relative fluctuations of the signal, as defined by Weiskoff [14], and by comparing this measure across different experimental conditions [6], [8]. Moreover, the evaluation of fMRI data in humans could provide an additional indirect assessment of compatibility issues of a stimulation device [4], [5]. In this case, several confounds, such as variability in subject response and/or physiological or movement-related signal changes, could affect the reproducibility of the results when looking at the effect on real data images.

Although these previous studies allow to evaluate the effect of devices on the acquisition quality in a qualitative or semiquantitative manner, they do not assess the statistical significance of the hypothesis of device compatibility. Here, we propose a novel, versatile, and automatic method for MR compatibility testing on gradient echo (GE) echo planar imaging (EPI) as acquired during a typical fMRI experiment. A statistical test on image sequences, acquired on a homogeneous phantom in different experimental conditions, is presented to evaluate changes in SNR values and time-domain standard deviations. Although the test is based on standard statistical tools and estimates of known image quality indexes, it represents, to our knowledge, the first attempt to exploit and integrate these elements in order to give the experimenters a statistically based approach to assess image quality for fMRI studies with mechatronic devices.

In this paper, the test is used to assess the compatibility of the proposed sensing glove. Functional studies on subjects performing a simple tactile task, with and without the sensing glove, are also performed. The reproducibility of the activated regions is estimated. An experiment that exploits information obtained from the sensing glove to build a model of expected BOLD time course is carried out and discussed.

## II. MATERIALS AND METHODS

### A. System Description

The prototype proposed here is a biomimetic sensing glove based on sensorized textile technology. Most of commercial devices are obtrusive, thus strongly affecting the natural movement and gesture of the hand. On the contrary, the glove used here is realized directly on a textile substrate and can be worn for a long time with no discomfort.

The sensors of the glove (Fig. 1) are made of a conductive elastomer (CE) material (commercial product provided by Wacker Ltd.) printed on a lycra/cotton fabric previously covered by an adhesive mask. The mask is designed according to the desired sensor and connection topology [16]. CE composites show piezoresistive properties when a deformation is applied [17]. CE materials represent an excellent tradeoff between transduction properties and possibility of integration in textiles, without af-

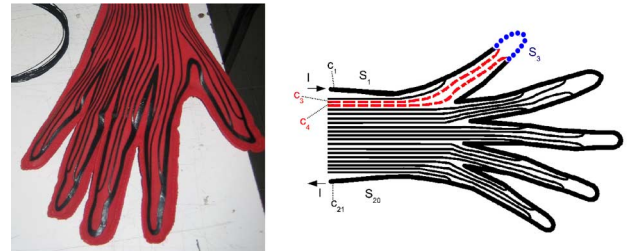


Fig. 1. Sensorized glove (left). Mask used for the sensing glove realization (right). The sensor  $S_3$  on the thumb (dotted line) and its connections (dashed lines) are pointed out.

flecting garment elasticity. Quasi-static and dynamical sensor characterization has been done in [18].

CE sensors exhibit some nonlinear dynamical properties and relatively long relaxation times [17] that should be taken into account during the formulation of the algorithm for the data interpretation.

Twenty sensors ( $S_1 - S_{20}$ ) are connected in series and they are represented by the wider lines of Fig. 1. Connections between sensors and electronic acquisition unit ( $C_1 - C_{21}$ ) are represented by the thinner line of Fig. 1. Sensors and connections are printed by using the same material, avoiding metallic wires on the joints. Moreover, by using this approach, the electrical contacts on the CE material can be placed in areas where the fabric deformations and stresses are reduced (e.g., the garment periphery).

Since connections are made by the same material as the sensors, they change their electrical resistance when the hand moves. For this reason, the acquisition unit front-end has been designed in order to compensate connection resistance variation. The sensor series is supplied with a constant current  $I$  and the voltage drops across consecutive connections are acquired using high-input impedance amplifiers (instrumentation amplifiers) following the methodology of [16]. When a finger is flexed, a deformation of the fabric occurs and the sensor is stretched. The sensor resistance changes and the instrumentation amplifier measures a voltage that is proportional to sensor resistance.

Let us consider the example of sensor  $S_3$ ; it is a sensor placed in the thumb finger area and is represented by the dotted line of Fig. 1 (right). Connections of this sensor are represented by the two dashed lines of Fig. 1 (right). If the amplifier is connected between  $C_3$  and  $C_4$ , only a little amount of current flows through interconnections with respect to the one that flows through  $S_3$ . In this way, if the current  $I$  is well dimensioned, the voltage read by the amplifier is almost equal to the voltage drop on the sensor that is proportional to the sample resistance. The current should be at least two orders of magnitude higher than those flowing in the connection lines, which are equal to the bias currents of the instrumentation amplifiers (approximately nanoamperes). The magnitude of the current is related to the sensor's impedance and limited by the current generator saturation.

The acquisition electronic unit is connected at the points  $C_1, C_2, \dots, C_{21}$ . This unit consists of a current generator and 20 instrumentation amplifiers. The current is injected between  $C_1$

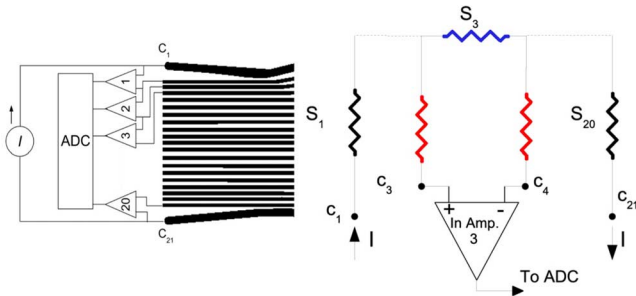


Fig. 2. Electronic acquisition unit and glove electrical model (left). Example of sensor  $S_3$  and its connection line (right).

and  $C_{21}$ , as shown in Fig. 2 (left). The instrumentation amplifiers are connected between consecutive interconnection points ( $C_1 - C_{21}$ ). Fig. 2 (right) shows the example of sensor  $S_3$  and its connection lines.

The current flowing through the sensors is lower than  $50 \mu\text{A}$ . A copper-shielded cable was used to connect the sensing glove to the acquisition electronics in the console room through a waveguide.

### B. Glove Data Interpretation

The basic concept of the proposed technology is that having a distribution of sensors around a joint to be monitored, it is possible to associate the sensor status (the set of the actual sensor values) to parameters related to finger movements. In terms of signal elaboration and data interpretation, several parameters can be extracted from the sensing glove depending on the quality of information needed by the application. Possible elaboration strategies are the following.

- 1) *Recognizing a discrete set of arm positions during user movements:* In a calibration phase, the sensor status can be acquired and stored for a set of relevant hand positions. In the detection phase, during subject movements, a suitable classifier can recognize the desired positions.
- 2) *Joint angles detection:* By using an external standard measurement system, the CE glove can be calibrated in order to identify a function that maps sensor status into hand joint angles. In the detection phase, the sensor signals are processed by the mapping function in order to obtain the desired joint angles.

In order to recognize a discrete set of hand postures, the system was calibrated by storing the sensor status for 32 hand positions. The data of the calibration dataset were used to design a classifier (based on Euclidean distance minimization algorithms) capable of recognizing the stored positions during natural user movements. Recognition results have been very encouraging, since the glove has recognized almost the 100% of the postures previously recorded if it was not removed from the hand. When the glove is removed and reworn, the sensor might be positioned in a different way with respect to the position used in the calibration phase. For this reason, the recognition percentage decreases to 95%. This problem can be solved with a postcalibration step that consists in acquiring the glove sensor status for the position of flat and closed hand.

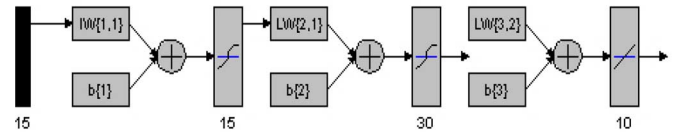


Fig. 3. Feedforward network applied to glove sensor data in order to obtain joint angles.

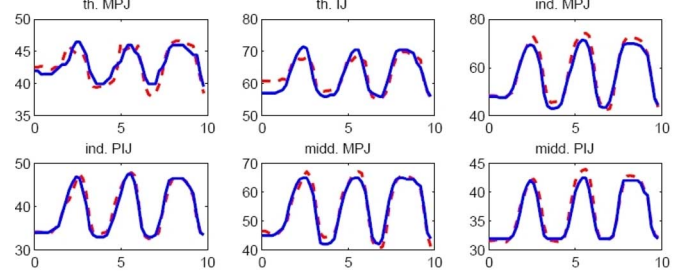


Fig. 4. Results of the application of the feedforward network algorithm. Dashed lines are the CE sensing glove outputs while continuous lines are Cyberglove outputs. Abscissa axis indicates the time expressed in seconds. Joints are indicated with the following: MPJ, metacarpophalangeal; IJ, trapeziometacarpal; PIJ, proximal interphalangeal. Fingers are indicated with the following: th., thumb; ind., index; midd., middle.

A more intelligent classifier, based on neural network techniques, has been designed in order to improve the performance after rewearing, and it has been tested with good results.

To extract joint angles from the glove signal, the Cyberglove (produced by Immersion Ltd.) was used to validate our system. The Cyberglove is realized by the application of electrogoniometers on fingers and it is used to measure hand joint angles. In our experiment, 15 glove sensors were used to measure the 10 hand DOFs.

During the calibration phase, the CE glove was worn by a subject together with the Cyberglove. The subject was asked to perform natural hand movements for about 1 min. Data from the CE glove and from the Cyberglove were simultaneously acquired and stored in a calibration dataset.

To obtain the desired map that transforms CE sensor values in hand joint angles, a feedforward neural network was trained using the backpropagation algorithm on the calibration dataset (after a suitable normalization, the CE sensors values were used as input and the Cyberglove outputs as targets).

The adopted network, reported in Fig. 3, has 15 tansigmoid input layers, 30 tansigmoid hidden layers, and 10 linear output layers.

In the test phase, the CE glove and the Cyberglove have been worn by the same subject during natural hand movements. Data coming from the CE glove have been processed by the obtained map and outputs have been compared with the ones produced by the Cyberglove.

Results have been encouraging, showing a maximum error less than 10%. Significant results related to six joints, obtained in a test trial, are reported in Fig. 4.

### C. fMRI Compatibility: Test of the System

1) *MR Compatibility Test*: For the design of every new device to be used inside the MR scanner environment during fMRI studies, safety and compatibility criteria must be satisfied and the interaction between MR primary components and mechatronic devices has to be considered [10], [19], [20].

An fMRI compatibility test is proposed for the system under investigation. The test employs mean differences of image quality indexes between different experimental conditions, i.e., with the device and a control condition without the device (baseline). The BOLD sensitive T2\*-weighted images are GE-EPI [echo time/repetition time (TE/TR) = 40/3000 ms, flip angle (FA) = 90°, bandwidth (BW) = 62.5 kHz, field of view (FOV) = 24 cm, number of slices = 25, 5-mm-thick axial slices, 1.5 T GE Scanner Excite HD] acquired using a spherical phantom of CuSO<sub>4</sub> solution.

The indexes proposed are the image SNR, estimated for each image in the time sequence, and the standard deviation, estimated for a group of image voxels (volume elements) in the center of the phantom. The SNR, corrected for different statistics of the noise in the phantom compared with the background noise [21], was defined as

$$\text{SNR} = \frac{P_{\text{center}}}{(1.53/4) \sum_{i=1}^4 \text{SD}_i} \quad (1)$$

where  $P_{\text{center}}$  is the mean value of a  $10 \times 10$  pixel area at the center of the image and  $\text{SD}_i$  is the mean standard deviation of the  $i$ th of four  $5 \times 5$  voxel ROIs areas at the image corners [21].

This operation was repeated for each image so that for each sequence, 20 estimates of the SNR were computed. The standard deviation of the image intensity time course was estimated in each image sequence: a  $15 \times 15$  voxel ROI located at the phantom center was used, resulting in 225 estimates of the standard deviation for each image sequence. The size of the selected ROI should be maximized to achieve a robust estimate. The actual ROI size was limited by the phantom cross section at first and last slices.

The test sets out to measure the differences between the means of the previous parameters, estimated from the images acquired under different experimental conditions and from those acquired with no device (reference images or baselines): SNR values were used to pinpoint image quality degradation, while time-domain standard deviations were compared in order to determine variances in the signal due to the devices.

Two image sequences (baselines I and II) without the device in the scanner room were acquired. An image sequence was acquired with the glove in the scanner room located at bore entrance (80 cm far from bore center) in two conditions: turned OFF, i.e., without power supply (glove OFF condition) and turned ON (glove ON condition). The shielded cables from the glove sensors to the acquisition systems, located in the console room, passed through the Faraday shield of the scanner room by means of a waveguide.

A  $z$ -test and a  $t$ -test were used for testing the differences in the mean values for the parameters outlined before: the former

test can be used when each sample is larger than 30, while the latter can be used if the sample size is smaller.

The hypothesis of the Gaussian distribution of the indexes must be satisfied for the statistical tests to be valid. The Kolmogorov–Smirnov (KS) test [22] can be used to verify the goodness of these hypotheses. We decided to implement a two-sided KS test, with a significance level equal to 0.05.

2) *Test on the Differences of Means for SNR Estimates*: An unpaired  $t$ -test was used to test SNR means difference estimated for two image sets [22]. The SNR was evaluated for 20 images acquired in each of the two experimental conditions to be compared, respectively, for baseline images and for images acquired with the device to be tested. A two-sided test was adopted with a significance level  $p$  equal to 0.05. An  $F$ -test to check the equality of the two sample-estimated variances has been performed [22]: in the hypothesis of equality of the variances, the previous reported  $p$ -value results in  $t$  critical values of  $t_c = \pm 2.024$ , with 38 DOF. When the absolute value of the  $t$ -statistic is greater than 2.024, the null hypothesis of equality of means can be rejected. In this case, if the test is applied to acquired sequences with the glove and reference, or baseline images, it is possible to assert that the device caused significant artifacts in the images.

3) *Test on Differences of Means for Time-Domain Standard Deviation Estimates*: A  $z$ -test was used in order to detect significant differences in the means of time-domain standard deviations estimated from two EPI image sequences. Since each sample is greater than 30 (225 estimates of the standard deviation for each image), the  $z$ -value can be thought as being normally distributed.

A two-sided test was adopted. The significance level for the null hypothesis was chosen as  $p = 0.05$ , resulting in critical values for the statistic given by  $z_c = \pm 1.96$  [22].

4) *Effects of the Scanning System on the Sensing Glove*: The effect of the imaging system on the signals acquired from the glove was investigated. The signal was acquired with the glove located at the scanner bore entrance, both while the scanner was not operating and while the system was scanning. To look at signal amplitude after a deformation is applied, glove signals were acquired when an operator was stretching the glove, by holding the two edges of the elastic fabric. This operation was performed during MR scanning. The contribution of noise introduced by the scanning system in the acquired signal was estimated using a power spectral density (PSD) analysis of the signal by means of a Welch-modified periodogram.

### D. fMRI Study Description

1) *fMRI Experiment*: Two fMRI sessions were performed on two right-handed healthy males (32- and 37-year olds, 1.7- and 1.85-m tall). Both volunteers signed informed consent for the test. Functional images with a GE-EPI (same scanning parameter as before) sequence and a spoiled grass 3-D T1-weighted anatomical image were acquired with a 1.5-T GE Scanner Excite HD. The subjects performed one hand finger tapping task following a blocked design paradigm alternating five times between 20 s of finger tapping task and 20 s of rest. Subject

1 used the left hand while subject 2 the right one. Two runs were performed by each subject wearing the glove and two runs without wearing the glove. Both subjects were trained before the session to keep a constant rate of finger tapping across each run. In a second experiment, the subjects were asked to perform a self-paced finger tapping task, where they had to decide autonomously the temporal patterns of finger movement.

2) *fMRI Data Processing*: The image data were spatially realigned to correct for head movements and spatially smoothed using a 3-mm full-width at half-maximum (FWHM) Gaussian kernel to increase image SNR. A multiple linear regression was performed: the regressor of interest was obtained by convolving the square wave describing the blocked paradigm with a model for the hemodynamic response function as in [23]. In the self-paced experiment, the expected response was obtained from the sensing glove signal: the information retrieved was about the temporal intervals while the subject was actually performing the task or he was still. A *t*-test on the coefficient of the regression pertaining the stimulus function was estimated. The maps were thresholded using an *F*-statistic. All the preprocessing steps and the analysis were performed with AFNI [24]. To test the effect of the wearable sensing glove on the fMRI maps, a reproducibility measure [25] was estimated, comparing the blocked design finger tapping task results, obtained with and without the glove. This reproducibility measure is defined as

$$R_{\text{overlap}}^{ij} = \frac{2V_{\text{overlap}}^{ij}}{V_i + V_j} \quad (2)$$

where  $V_i$  and  $V_j$  are the sizes of activated volumes in the  $i$ th and  $j$ th scan, respectively, while  $V_{\text{overlap}}^{ij}$  is the size of the volume activated in both scans.

### III. RESULTS

#### A. fMRI Compatibility Test Results

1) *Effect of the Sensing Glove on the Images*: Test results are summarized in Table I. The KS test revealed that both SNR and time-domain standard deviation values are Gaussian-distributed for all samples. The *F*-test on the equality of variances showed no significant differences in all examined cases. The compatibility test showed a mild effect of the system on image quality.

Changes in image quality are present as regards time-domain standard deviation in two slices, while others seem to be unaffected. No significant difference was found in SNR values across different experimental conditions.

Slices labeled with lower numbers are those closer to bore entrance.

2) *Effects of the Scanning System on the Sensing Glove*: In Fig. 5, the PSD of the acquired signal under different experimental conditions is shown. These data show that the scanner causes a relevant noise power on the acquired signal. The PSD of the signal from a glove sensor is shown. The signal PSD is much larger than the noise for frequencies below 5 Hz. A low-pass filtering operation (Butterworth order 12, cutoff frequency 5 Hz) allowed to filter scanner noise (data not shown).

TABLE I  
GLOVE COMPATIBILITY TEST RESULTS

| Experiment     | Slice #1 |                  | Slice #5 |         | Slice #10 |         | Slice #20 |                  |
|----------------|----------|------------------|----------|---------|-----------|---------|-----------|------------------|
|                | t SNR    | z SD             | t SNR    | z SD    | t SNR     | z SD    | t SNR     | z SD             |
| Baseline I vs  | -0.79    | 1.28             | 0.84     | 0.73    | 0.03      | 0.12    | 0.39      | -0.15            |
| Baseline II    | [0.436]  | [0.201]          | [0.406]  | [0.465] | [0.976]   | [0.905] | [0.699]   | [0.881]          |
| Baseline I vs  | -0.68    | 0.53             | -1.54    | 1.40    | -0.22     | 0.77    | -0.74     | 1.18             |
| Glove off      | [0.501]  | [0.596]          | [0.131]  | [0.162] | [0.827]   | [0.441] | [0.464]   | [0.238]          |
| Baseline II vs | 0.1      | <b>-2.8</b>      | -0.75    | 0.8     | -1.23     | 1.37    | -0.27     | <b>2.22</b>      |
| Glove off      | [0.921]  | [ <b>0.005</b> ] | [0.458]  | [0.424] | [0.226]   | [0.171] | [0.789]   | [ <b>0.026</b> ] |
| Baseline I vs  | -1.25    | -1.05            | -0.09    | -0.91   | -0.16     | -0.26   | -0.21     | -0.14            |
| Glove on       | [0.219]  | [0.294]          | [0.929]  | [0.363] | [0.874]   | [0.795] | [0.839]   | [0.888]          |
| Baseline II vs | -0.58    | <b>-2.4</b>      | -1.04    | -0.23   | -0.44     | -1.23   | 0.44      | -0.67            |
| Glove on       | [0.565]  | [ <b>0.016</b> ] | [0.305]  | [0.818] | [0.662]   | [0.219] | [0.662]   | [0.503]          |

Critical values:  $t = \pm 2.024$ ,  $z = \pm 1.96$ . Values outside the acceptance region are shown in bold. Corresponding *p*-values are shown in brackets.

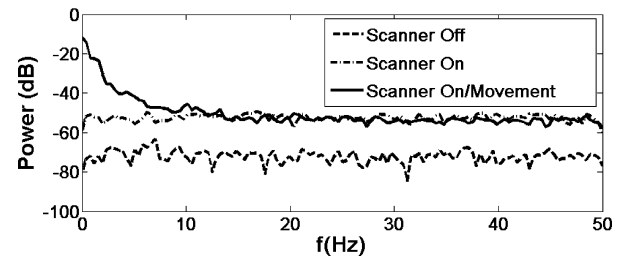


Fig. 5. PSD of the signals acquired from the sensing glove under different experimental conditions.

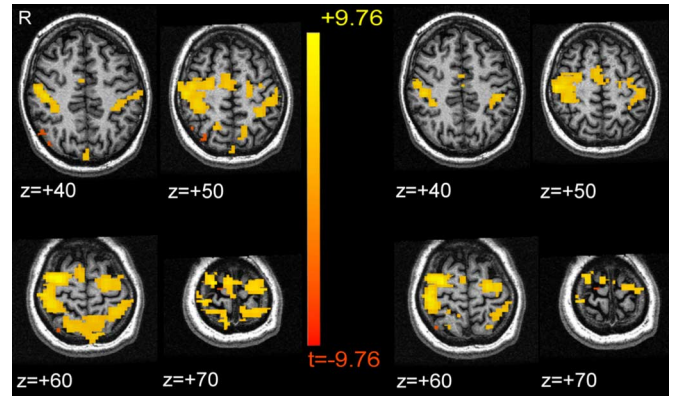


Fig. 6. fMRI results for subject 1 (Talairach space). Task: block-designed finger tapping (threshold  $F$ ,  $p < 10^{-7}$ ) without the glove (left) and with the glove (right).

#### B. fMRI Study Results

In Fig. 6, functional maps of the finger tapping task for one subject are shown. In the left part, the maps of the experiment without the glove are shown, while the right part depicts the results of the experiment with the glove. The *t*-statistic regarding the regressor of interest coefficient is shown superimposed on an anatomical image in Talairach space. Only those voxels with  $p$ -value  $< 10^{-7}$  are shown.

Significant activations were found in areas that are likely to be involved in the task under examination, in both cases. Activations were found in the ipsilateral and contralateral primary motor cortex and supplementary motor area (SMA). Right and



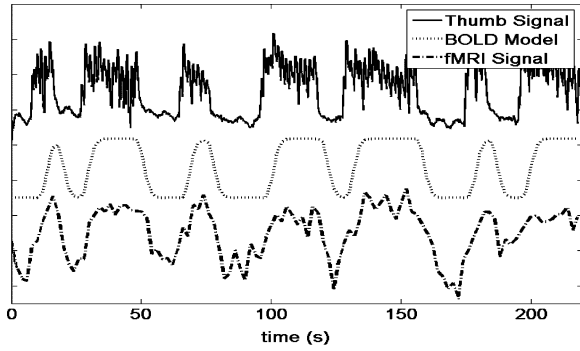


Fig. 7. Signal acquired from a glove sensing element at the index (upper graph) and expected hemodynamic response (middle graph) estimated from the sensing glove information. Actual time series extracted from the contralateral primary motor cortex (M1) subject 1 (lower graph).

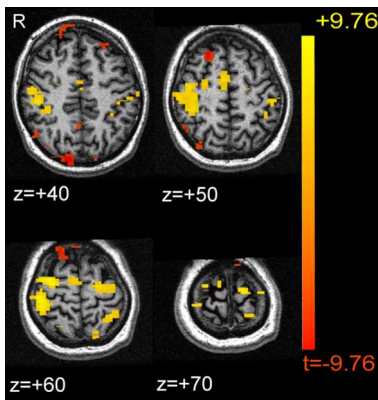


Fig. 8. fMRI results in Talairach coordinates for subject 1. Task: self-paced finger tapping (threshold  $F, p < 10^{-5}$ ).

left precuneus, inferior frontal gyrus, and posterior parietal areas were activated as well.

The reproducibility measures estimated for the two subjects were, respectively, 64% (shown results) and 63% (results not shown).

In Table II, the Talairach coordinates of local  $F$ -score maxima of suprathreshold brain areas are reported for the two subjects. The results resulting from analysis data related to finger tapping task in two experimental conditions, with the subjects wearing the glove and without wearing the glove, are shown.

In the upper part of Fig. 7, the raw data acquired from a glove sensor, at the index finger, during the self-paced finger tapping experiment are shown. These data were used to extract the start and the end of each movement-related intervals. This information was used to build a squared wave that was convolved with a hemodynamic response function to obtain an expected time course of activation, i.e., the regressor of interest (Fig. 7, middle graph).

The MRI signal extracted from an activated region is shown in Fig. 7 (lower graph). The activation maps obtained are shown in Fig. 8 (threshold  $F$ -statistics,  $p < 10^{-5}$ ). Ipsilateral and contralateral primary motor cortices and SMA and posterior parietal areas were found activated.

#### IV. DISCUSSION

In this paper, an fMRI-compatible glove, realized by means of strain sensing fabric, was described. This device can be used to monitor hand posture and gesture in functional studies. This information could be integrated with the fMRI data in order to explore brain networks involved in the execution of tactile or motor tasks.

Virtual reality or enhanced mixed scenarios can be designed for fMRI studies on complex motor and behavioral tasks as those related to person-to-person interaction (i.e., handshake, sign language) or person to object (grip, objects manipulation).

The glove can be used to evaluate and validate visuohaptic devices, as those used for telesurgery, by correlating subjective reports about their effectiveness with objective measures, as brain activity highlighted by fMRI.

In this paper, after describing the proposed glove and its possible applications, a test to assess the compatibility of devices with fMRI investigations has been introduced.

The methods proposed in literature do not offer the experimenter the possibility to adopt a statistically based approach for accepting or rejecting the hypothesis of device compatibility.

A statistical test is introduced to evaluate changes in SNR values and time-domain standard deviations in automatically selected ROIs of image sequences across different experimental conditions. It is very important to verify, i.e., by means of the KS test, the hypothesis of Gaussian distribution of these index estimates in order for the compatibility test to be valid.

The choice of using typical GE-EPI images is motivated by the need for testing the compatibility specifically for fMRI experiments.

Different sources of variability have been taken into account in designing this compatibility test. Interobserver variability has been minimized by using an automatic method for ROI selection: the regions used for the computation of signal intensity for the estimation of SNR and for time-domain standard deviation are selected in the center of the phantom, while the ROIs for the computation of noise level, in the estimation of SNR, are chosen at the image borders. ROI location and extension are chosen to avoid the inclusion of phantom borders in the calculation. The variability due to the positioning of the phantom in the magnet does not alter the test results since the reference image sequence is acquired in the same test session as the one to be tested. Comparing image sequences in the same scanning session, moreover, is important since changes in the MRI scanner from session to session are avoided. As previously reported, system instabilities may cause the SNR to vary over time [26]. These changes may, in fact, represent a confounder in the compatibility evaluation.

To test for short-term system variabilities, more baseline scans are acquired in the same scanning session. No significant differences were outlined among reference images acquired on the same day.

The effect of the device entering the MR setting was investigated across image sequences and not between single images under different experimental conditions in order to look for time-varying effects of the devices on the image quality.

The proposed test was applied to a 1.5-T scanner, but should be independent from the particular scanner and from the main

TABLE II  
TALAIRACH ATLAS COORDINATES OF LOCAL  $F$ -SCORE MAXIMA DURING FINGER TAPPING TASK

| Brain Areas                | Hemisphere | Subj. #1 |     |    |       |     |     | Subj. #2 |     |    |       |     |    |
|----------------------------|------------|----------|-----|----|-------|-----|-----|----------|-----|----|-------|-----|----|
|                            |            | No Glove |     |    | Glove |     |     | No Glove |     |    | Glove |     |    |
|                            |            | x        | y   | z  | x     | y   | z   | x        | y   | z  | x     | y   | z  |
| Precentral Gyrus           | L          | -31      | -21 | 60 | -32   | -20 | 60  | -33      | -26 | 59 | -33   | -26 | 60 |
|                            | R          | 34       | -11 | 59 | 33    | -10 | 59  | 27       | -11 | 50 | 26    | -11 | 50 |
| Postcentral Gyrus          | L          | -39      | -29 | 56 | -38   | -28 | 55  | -37      | -29 | 57 | -38   | -28 | 57 |
|                            | R          | 33       | -34 | 54 | 36    | -33 | 55  | 47       | -25 | 47 | 48    | -25 | 48 |
| Medial Frontal Gyrus (SMA) | L          | -5       | -7  | 49 | -3    | -11 | 49  | -3       | -9  | 51 | -3    | -9  | 50 |
|                            | R          | 4        | -12 | 50 | 3     | -12 | 50  | 5        | -8  | 49 | 3     | -11 | 50 |
| Inferior Frontal Gyrus     | L          |          |     |    |       |     |     | -56      | 6   | 28 | -58   | 7   | 27 |
|                            | R          | 56       | 16  | 10 | 57    | 15  | 10  | 56       | 9   | 32 | 58    | 12  | 31 |
| Superior Parietal Lobule   | L          | -36      | -55 | 53 | -34   | -55 | 52  |          |     |    |       |     |    |
|                            | R          | 23       | -48 | 60 | 30    | -46 | 60  | 22       | -67 | 55 | 22    | -65 | 54 |
| Inferior Parietal Lobule   | L          | -40      | 48  | 41 | -40   | -48 | -41 | -41      | -38 | 50 | -42   | -38 | 49 |
|                            | R          | 33       | -38 | 53 | 37    | -39 | 53  | 50       | -32 | 42 | 47    | -31 | 42 |
| Precuneus                  | L          | -18      | -70 | 42 | -18   | -71 | 42  |          |     |    |       |     |    |
|                            | R          | 18       | -62 | 45 | 17    | -63 | 45  | 21       | -65 | 51 | 21    | -65 | 51 |

Talairach atlas coordinates (LPI orientation) of local  $F$ -score maxima are reported for subject 1 (Subj. 1) and subject 2 (Subj. 2) observed in the finger tapping task. Two experimental conditions are reported for each subject: finger tapping without the glove (No Glove) and finger tapping with the glove (Glove).

field value, the main reason obviously being that the reference image sequence is acquired with the same scanner.

The compatibility test results of the sensing glove showed that the system slightly affects GE-EPI image quality. These small effects are also present when the system is turned OFF, seem not to be homogeneous, and do not affect all the phantom slices. The effects of the system we tested cannot be detected by visual inspection. The images SNRs seem not to be affected while some changes are highlighted in the time-domain standard deviation.

Some improvements may still be applied to the system such as an effective shielding of the wires as they are connected to the CE. Moreover, a shielding of the sensor network may be designed.

The tests with the phantom were performed with the glove located 80 cm from the bore center. This position is representative of normal device operation, taking into account 1.7 m as subject height. In case of shorter subjects, the device compatibility test should be performed again, moving the device closer to the imaging volume.

The noise introduced by the scanning system is relevant: to stress this point, signals from the glove located at the scanner bore entrance were acquired, both while the scanner was not operating and while the system was scanning. To look at signal amplitude after a deformation is applied, an operator stretched the glove, by holding the two edges of the elastic fabric. The movements were mainly characterized by low-frequency components (<5 Hz). The power of this signal was higher than noise power and the signal shape could be easily retrieved using a low-pass filter.

Functional studies on human subjects have also been performed, mainly to verify the test results previously obtained with the phantom. The activated regions found in both the experiments, with and without the glove, are consistent with those expected in a blocked design finger tapping experiment [27]. As described in literature, brain activation during finger movement was found in the contralateral and ipsilateral primary motor cortex (M1), SMA, the premotor cortex of both hemispheres, and the contralateral somatosensory cortex [27], [28]. Consis-

tent with literature results, ipsilateral M1 activation was found to be significantly smaller than the contralateral one. The estimated reproducibility measures indicate an acceptable similarity degree between the activated regions found with and without wearing the sensing glove [29] confirming the compatibility test results. The reproducibility measures in fact were compared to those found in literature: a within-session reproducibility value in the range of  $74 \pm 7\%$  for the overlapping volume has been found for visual activation patterns. These values were obtained with a  $4 \text{ mm} \times 4 \text{ mm} \times 5 \text{ mm}$  FWHM Gaussian filter and were shown to increase along with the filter width. The same values with no filter applied were around 60%. It is worth noting that there are many factors that may alter the value of this index, as small differences in the task, habituation, and learning phenomena. Moreover, this index was shown to change with brain areas [30]. Another confounding factor may be represented by changes in the movement rate [31]. These factors were minimized by training our volunteers to keep a constant rate of finger tapping. Moreover, the short execution period of the task likely excludes any effect such as being tired or annoyed.

The results shown in Table II confirm a good reproducibility of activated brain areas within each subject. The differences between the brain areas found in the two subjects can be related to between-subjects variability and also to the differences in the task performed by the subjects. It is very important to point out that our goal was to check whether the system does affect the reproducibility of fMRI results within each subject, and a comparison of the activated areas between the two subjects is beyond the scope of this paper.

The subjects also performed a self-paced finger tapping experiment. In this test, only a small part of the available information acquired with the sensing glove was used for fMRI data analysis and used to reconstruct the actual timing of the subject's overall movement.

We have to highlight that the self-paced experiment is not optimal for the statistical power and a lower  $F$ -statistic threshold is used for displaying self-paced task-related results, as compared to the block design. The activated regions are consistent with a pattern found in finger tapping experiments for both subjects.

## V. CONCLUSION

In this paper, a sensing glove made of strain sensing fabric was described. To assess the possibility of using the glove in fMRI studies, a compatibility test was introduced. The test can be used for mechatronic devices to be used within an MR environment in order to evaluate artifacts caused by their presence and actuation. The test was developed specifically for the compatibility of devices to be used during an fMRI study. Unlike previously reported tests, it allows to assess the statistical significance of the compatibility of the device and is completely automatic. Moreover, it can be applied to the same kind of image sequence used for fMRI investigations. The test is developed to be applied to image sequences acquired using a phantom.

The glove has shown a good compatibility with fMRI studies, both in phantoms and subjects tests. The possibility of retrieving information from the glove, without affecting image quality, may allow to employ the system for hand posture and hand gesture monitoring during an fMRI experiment.

In addition to hand posture and gesture recognition, next developments aim at enabling the sensing glove to record haptic interaction signals. Further research has to be done in order to improve MRI compatibility of the system.

## ACKNOWLEDGMENT

The authors wish to thank the MRI Laboratory at the IFC-CNR, Pisa, Italy, coordinated by M. Lombardi.

## REFERENCES

- [1] VRLOGIC GmbH. Cyberglove. (2008, May). [Online]. Available: <http://www.vrlogic.com/html/immersion/cyberglove.html>
- [2] K. J. Friston, A. P. Holmes, K. J. Worsley, J. B. Poline, C. D. Frith, and R. S. J. Frackowiak, "Statistical parametric maps in functional imaging: A general linear approach," *Hum. Brain Mapp.*, vol. 2, pp. 189–210, 1995.
- [3] Fifth Dimension Technologies. 5DT Data Glove 5 MRI/5DT Data Glove 16 MRI. (2008, May). [Online]. Available: <http://www.5dt.com/products/pdataglovemri.html>
- [4] J. Hidler, T. Hodics, B. Xu, B. Dobkin, and L. G. Cohen, "MR compatible force sensing system for real-time monitoring of wrist moments during fMRI testing," *J. Neurosci. Methods*, vol. 155, pp. 300–307, 2006.
- [5] J. Z. Liu, T. H. Dai, T. H. Elster, V. Sahgal, R. W. Brown, and G. H. Yue, "Simultaneous measurement of human joint force, surface electromyograms, and functional MRI-measured brain activation," *J. Neurosci. Methods*, vol. 101, pp. 49–57, 2002.
- [6] J. Reithler, H. Reithler, E. Van Den Boogert, R. Goebel, and H. van Mier, "Resistance-based high resolution recording of predefined 2-dimensional pen trajectories in an fMRI setting," *J. Neurosci. Methods*, vol. 152, pp. 10–17, 2006.
- [7] M. Tada and T. Kanade, "An MR compatible optical force sensor for human function modeling using MRI," in *Proc. MICCAI* (Lecture Notes in Computer Science), 2004, vol. 3217, pp. 129–136.
- [8] G. A. James, G. He, and Y. Liu, "A full-size MRI-compatible keyboard response system," *NeuroImage*, vol. 25, pp. 328–331, 2005.
- [9] R. Gassert, R. Moser, E. Burdet, and H. Bleuler, "MRI/fMRI-compatible robotic system with force feedback for interaction with human motion," *IEEE ASME Trans. Mechatronics*, vol. 11, no. 2, pp. 216–224, Apr. 2006.
- [10] Food and Drug Administration. (1997, Feb. 7). *A Primer on Medical Device Interactions with Magnetic Resonance Imaging Systems*, U.S. Department of Health and Human Services, Center for Devices and Radiological Health, Eds. Magnetic Resonance Working Group Draft [Online]. Available: <http://www.fda.gov/cdrh/ode/primerf6.html>
- [11] K. Chinzei, R. Kikinis, and F. A. Jolesz, "MR compatibility of mechatronic devices: Design criteria," (Lecture Notes in Computer Science 1679), in *Book of Abstracts: Proc. MICCAI 1999*. Cambridge, U.K.: Springer-Verlag, pp. 1020–1031.
- [12] B. A. Schueler, T. B. Parrish, J. C. Lin, B. E. Hammer, B. J. Pangrle, E. R. Ritenour, J. Kucharczyk, and C. L. Truweit, "MRI compatibility and visibility assessment of implantable medical devices," *J. Magn. Reson. Imag.*, vol. 9, pp. 596–603, 1999.
- [13] A. Guermazi, Y. Miaux, S. Zaim, C. G. Peterfy, D. White, and H. K. Genant, "Metallic artifacts in MR imaging: Effects of main field orientation and strength," *Clin. Radiol.*, vol. 58, pp. 322–328, 2003.
- [14] R. M. Weisskoff, "Simple measurement of scanner stability for functional NMR imaging of activation in the brain," *Magn. Reson. Med.*, vol. 36, pp. 643–645, 1996.
- [15] NEMA Standards Publication MS 1-2001. (2007, Feb. 28). [Online]. Available: [http://www.nema.org/stds/complimentary-docs/upload/MS\\_1.pdf](http://www.nema.org/stds/complimentary-docs/upload/MS_1.pdf)
- [16] A. Tognetti, F. Lorussi, R. Bartalesi, S. Quaglini, M. Tesconi, G. Zupone, and D. De Rossi. (2005, Mar.). Wearable kinesthetic system for capturing and classifying upper limb gesture in post-stroke rehabilitation. *J. Neuroeng. Rehabil.* [Online]. 2(8). Available: <http://www.jneuroengrehab.com/content/2/1/8>
- [17] W. Peng, X. Feng, D. Tianhuai, and Q. Yuanzhen, "Time dependence of electrical resistivity under uniaxial pressures for carbon black/polymer composites," *J. Mater. Sci.*, vol. 39, no. 15, pp. 4937–4939, 2004.
- [18] F. Lorussi, E. P. Scilingo, M. Tesconi, A. Tognetti, and D. De Rossi, "Strain sensing fabric for hand posture and gesture monitoring," *IEEE Trans. Inf. Technol. Biomed.*, vol. 9, no. 3, pp. 372–381, Sep. 2005.
- [19] J. F. Schenck, "Safety of strong, static magnetic fields," *J. Magn. Reson. Imag.*, vol. 12, pp. 2–19, 2000.
- [20] K. M. Ludeke, P. Roschmann, and R. Tischler, "Susceptibility artefacts in NMR imaging," *Magn. Reson. Med.*, vol. 3, pp. 329–343, 1985.
- [21] J. Sijbers, A. J. Den Dekker, J. Van Audekerke, M. Verhoye, and D. Van Dyck, "Estimation of the noise in magnitude MR images," *Magn. Reson. Imag.*, vol. 16, pp. 87–90, 1998.
- [22] I. M. Chakravarti, R. G. Laha, and J. Roy, *Handbook of Methods of Applied Statistics, vol. 1*. Chichester, U.K.: Wiley, 1967.
- [23] M. S. Cohen, "Parametric analysis of fMRI data analysis using linear system methods," *Neuroimage*, vol. 6, pp. 93–103, 1997.
- [24] R. W. Cox, "AFNI: Software for analysis and visualization of functional magnetic resonance neuroimages," *Comput. Biomed. Res.*, vol. 29, pp. 162–173, 1996.
- [25] S. A. R. B. Rombouts, F. Barkhof, F. G. C. Hoogenraad, M. Sprenger, J. Valk, and P. Scheltens, "Test-retest analysis of the activated areas in the human visual cortex using functional MRI imaging," *Amer. J. Neuroradiol. (AJNR)*, vol. 18, pp. 1317–1322, 1997.
- [26] K. R. Thulborn, "Quality assurance in clinical and research echo planar functional MRI," in *Functional MRI*, P. A. Bandettini and C. T. W. Moonen, Eds. Berlin, Germany: Springer-Verlag, 2000, pp. 337–346.
- [27] S. M. Rao, J. R. Binder, P. A. Bandettini, T. A. Hammeke, F. Z. Yetkin, A. Jesmanowicz, L. M. Lisk, G. L. Morris, W. M. Mueller, L. D. Estkowski, E. C. Wong, V. M. Haughton, and J. S. Hyde, "Functional magnetic resonance imaging of complex human movements," *Neurology*, vol. 43, no. 11, pp. 2311–2318, 1993.
- [28] H. Boecker, A. Kleinschmidt, M. Requardt, W. Hanicke, K. D. Merboldt, and J. Frahm, "Functional cooperativity of human cortical motor areas during self-paced simple finger movements. A high-resolution MRI study," *Brain*, vol. 117, pp. 1231–1239, 1994.
- [29] S. A. R. B. Rombouts, F. Barkhof, F. G. C. Hoogenraad, M. Sprenger, J. Valk, and P. Scheltens, "Within-subject reproducibility of visual activation patterns with functional magnetic resonance imaging using multislice echoplanar imaging," *Magn. Reson. Imag.*, vol. 16, pp. 105–113, 1998.
- [30] W. C. M. Machielsens, S. A. R. B. Rombouts, F. Barkhof, P. Scheltens, and M. P. Witter, "fMRI of visual encoding: Reproducibility of activation," *Hum. Brain Mapp.*, vol. 9, pp. 156–164, 2000.
- [31] S. M. Rao, P. A. Bandettini, J. R. Binder, J. A. Bobholz, T. A. Hammeke, E. A. Stein, and J. S. Hyde, "Relationship between finger movement rate and functional magnetic resonance signal change in human primary motor cortex," *J. Cereb. Blood Flow Metab.*, vol. 16, pp. 1250–1254, 1996.



**Nicola Vanello** was born in Carrara, Italy, on June 12, 1972. He received the M.Sc. degree in electronic engineering and the Ph.D. degree in bioengineering from the University of Pisa, Pisa, Italy, in 2001 and 2006, respectively.

He is currently an Assistant Professor in the Department of Information Engineering, University of Pisa. His current research interests include functional MRI (fMRI) experimental design and data analysis and biomedical signal processing.





**Valentina Hartwig** was born in Livorno, Italy, on April 12, 1977. She received the M.Sc. degree in electronic engineering in 2003 from the University of Pisa, Pisa, Italy, where she is currently working toward the Ph.D. degree in bioengineering in the Faculty of Engineering.

At the University of Pisa, she is engaged in numerical simulation of MR electromagnetic field and biological tissues interaction. She is the author or coauthor of a number of papers and international conference proceedings about MR compatibility test and design of mechatronic devices.

design of mechatronic devices.



**Mario Tesconi** received the Graduate degree in biomedical electronic engineering and the Ph.D. degree in robotics, automation, and bioengineering from the University of Pisa, Pisa, Italy, in 2001 and 2007, respectively.

He is currently with the Interdepartmental Research Center "E. Piaggio," University of Pisa. His current research interests include the design and development of wearable devices for biomechanical and multimedia application, which are predominantly focused on lower limb biomechanics with a specific

study on the design and realization of a knee sleeve able to detect the posture and movement of the knee joint.



**Emiliano Ricciardi** received the Ph.D. degree in neurosciences from the Scuola Superiore "Sant'Anna," Pisa, Italy.

He studied medicine at the University of Pisa. Since 1998, he has spent more than four years at the National Institutes of Mental Health, Bethesda, MD, where he acquired expertise in the *in vivo* brain functional exploration methodologies. He is currently an Assistant Professor of clinical biochemistry at the Laboratory of Clinical Biochemistry and Molecular Biology, University of Pisa Medical School, Pisa. His

current research interests include cognitive neuroscience with focus on how the brain perceives and recognizes the external environment.



**Alessandro Tognetti** received the Graduate degree in electronic engineering and the Ph.D. degree in robotics, automation, and bioengineering from the University of Pisa, Pisa, Italy, in 2001 and 2005, respectively.

He is currently a Postdoctoral Researcher at the Interdepartmental Research Center "E. Piaggio," University of Pisa, where he is engaged in the design and development of wearable kinesthetic interfaces for human posture and movement detection. He is the author or coauthor of several papers and has contributed to international conferences and chapters in international books. His

current research interests include sensor design and signal and information processing.



**Giuseppe Zupone** was born in Taranto, Italy, on January 17, 1971. He received the Graduate degree in biomedical electronic engineering from the Faculty of Engineering, University of Pisa, Pisa, Italy, in 2003.

He is currently engaged in research at the Interdepartmental Research Center "E. Piaggio," University of Pisa.

Mr. Zupone is the winner of a grant at the Interdepartmental Research Center "E. Piaggio," University of Pisa on the characterization of wearable strain sensors, related to the European research project "MyHeart."



**Roger Gassert** (S'02–M'06) was born in 1976. He received the M.S. degree in microengineering and the Ph.D. degree in robotics from the Ecole Polytechnique Federale de Lausanne (EPFL), Lausanne, Switzerland, in 2002 and 2006, respectively.

He is currently a Postdoctoral Fellow in the Department of Bioengineering, Imperial College London, London, U.K., where he is engaged in research on techniques for functional MRI (fMRI) compatible robotic devices to interact with human motion. His current research interests include assistive

devices, medical robotics, and neuroscience.



**Dominique Chapuis** (M'04) received the M.Sc. degree in microengineering in 2003 from the Ecole Polytechnique Fédérale de Lausanne (EPFL), Lausanne, Switzerland, where he is currently working toward the Ph.D. degree at the Laboratoire de Systèmes Robotiques (LSRO).

His current research interests include medical robotics, haptic interfaces, and actuators.



**Nicola Sgambelluri** was born in Locri, Italy, in 1975. He received the M.Sc. degree in electronic engineering from the University of Pisa, Pisa, Italy, in 2002, and the Ph.D. degree in automation, robotics, and bioengineering from the Department of Electrical System and Automation (DSEA), in 2006.

He is currently with the Interdepartmental Research Center "E. Piaggio," University of Pisa. His current research interests include design and realization of immersive and nonimmersive haptic interfaces for virtual reality, based on magnetorheological (MR) fluids.



**Enzo P. Scilingo** received the Laurea degree in electronic engineering from the University of Pisa, Pisa, Italy, in 1995, and the Ph.D. degree in bioengineering from the University of Milan, Milan, Italy, in 1998.

He was a Postdoctoral Fellow with the Italian National Research Council for two years. He is currently an Assistant Professor in the Department of Information Engineering, University of Pisa, where he is engaged in research at the Interdepartmental Research Center "E. Piaggio." He is the author of several papers, and has contributed to international conferences

and chapters in international books. His current research interests include haptic interfaces, biomedical and biomechanical signal processing, modeling, control, and instrumentation.



**Giulio Giovannetti** was born in Livorno, Italy, on July 6, 1970. He received the degree in electronic engineering and in biomedical engineering in 2000 and 2004, respectively, from the University of Pisa, Pisa, Italy, where he is currently working toward the Ph.D. degree in bioengineering in the Faculty of Engineering.

Since 2000, he has been a Researcher at the MRI Laboratory, Istituto di Fisiologia Clinica, Consiglio Nazionale delle Ricerche (CNR), Pisa. He is the author or coauthor of a number of papers on simulation

and design of MR coils and hardware, and has also contributed to proceedings.



**Vincenzo Positano** (M'98) received the degree in electronic engineering from the University of Pisa, Pisa, Italy, in 1992.

He is currently a Researcher at the Istituto di Fisiologia Clinica (IFC), Consiglio Nazionale delle Ricerche (CNR), Pisa. His current research interests include developing innovative algorithms for image analysis and image fusion, in particular, in the cardiac MRI field.



**Maria F. Santarelli** received the M.Sc. degree in information science and the Ph.D. degree in biomedical engineering from the University of Pisa, Pisa, Italy, in 1987 and 1993, respectively.

She teaches regular courses on medical informatics and programming in the Department of Biomedical Engineering, University of Pisa. She is currently a Senior Researcher at the MRI Laboratory, Istituto di Fisiologia Clinica, Consiglio Nazionale delle Ricerche (CNR), Pisa. She is the author or coauthor of a number of papers, proceedings, and books

on medical image processing and tissue characterization. Her current research interests include biomedical signal and image processing.



**Antonio Bicchi** (S'87–M'89–SM'99–F'06) received the Graduate degree from the University of Bologna, Bologna, Italy, in 1988.

Between 1988 and 1990, he was a Postdoctoral Scholar at the Massachusetts Institute of Technology A.I. Laboratory, Cambridge. He is currently a Professor of automatic control and robotics at the Interdepartmental Research Center "E. Piaggio," University of Pisa, Pisa, Italy. He is the author or coauthor of more than 200 papers in international journals, books, and refereed conferences proceedings. He has

also been an Editor for several scientific journals. His current research interests include dynamics, kinematics, and control of complex mechanical systems, and theory and control of nonlinear systems.

Prof. Bicchi is the Vice President for Member Activities of the IEEE Robotics and Automation Society (RAS). He has also been an IEEE-RAS Distinguished Lecturer and the Chairman of conferences such as WorldHaptics in 2005 and Hybrid Systems: Computation and Control in 2007.



**Pietro Pietrini** received the Ph.D. degree in neurosciences from the Scuola Superiore "Sant'Anna," Pisa, Pisa, Italy.

He has spent over a decade at the National Institutes of Health, Bethesda, MD, and currently collaborates actively with several national and international research groups. He is currently a Professor of clinical biochemistry and the Director of the Laboratory of Clinical Biochemistry and Molecular Biology, University of Pisa Medical School, Pisa. He is the author or coauthor of more than 150 papers in peer-reviewed

journals, and has received several national and international grants. His current research interests include the *in vivo* study of the neurometabolic bases of cognition and behavior in humans in physiological conditions and during neuropsychiatric disorders by using *in vivo* brain functional methodologies in combination with neuropsychological tasks.



**Danilo De Rossi** received the Laurea degree in chemical engineering from the University of Genoa, Genoa, Italy, in 1976.

From 1976 to 1981, he was a Researcher at the Istituto di Fisiologia Clinica, Consiglio Nazionale delle Ricerche (CNR), Pisa, Italy. He was also engaged in teaching and research in Australia, Brazil, France, Japan, and the USA. In 1982, he joined the Faculty of Engineering, University of Pisa, Pisa, where he is currently a Full Professor of bioengineering at the Interdepartmental Research Center "E.

Piaggio." He is the author or coauthor of more than 270 peer-reviewed papers in international science journals and peer-reviewed proceedings, a coinventor of 14 patents, and a coauthor of eight books. His current research interests include the physics of organic and polymeric materials, and the design of sensors and actuators for bioengineering and robotics.



**Luigi Landini** was born in La Spezia, Italy, on October 31, 1949. He received the M.Sc. degree in physics from the University of Pisa, Pisa, Italy, in 1974.

Since 1992, he has been teaching regular courses on biomedical signal and image processing in the Department of Electronic Engineering, University of Pisa, where he is currently a Full Professor of biomedical engineering in the Faculty of Engineering, where he is also engaged in research on biomedical engineering in the Department of Information Engineering. He is the author or coauthor of more than 200 reports and papers on ultrasonic tissue characterization, digital signal, magnetic resonance image processing, and medical imaging.